Panchromatic averaged stellar populations

R. Riffel,[1]⋆ C. Bonatto,[1] R. Cid Fernandes,[2] M. G. Pastoriza[1] and E. Balbinot[1]

[1]*Departamento de Astronomia, Universidade Federal do Rio Grande do Sul. Av. Bento Gonçalves 9500, 91501-970 Porto Alegre, RS, Brazil*
[2]*Departamento de Física – CFM – Universidade Federal de Santa Catarina, 88010-970 Florianópolis, SC, Brazil*

ABSTRACT

We study how the spectral fitting of galaxies, in terms of light fractions, derived in one spectral region translates into another region, by using results from evolutionary synthesis models. In particular, we examine propagation dependencies on evolutionary population synthesis (EPS) models (GRASIL, GALEV, Maraston and GALAXEV), age, metallicity and stellar evolution tracks over the near-ultraviolet–near-infrared (NUV–NIR, 3500 Å to 2.5 μm) spectral region. Our main results are as follows: as expected, young ($t \lesssim 400\,\mathrm{Myr}$) stellar population fractions derived in the optical cannot be directly compared to those derived in the NIR, and vice versa. In contrast, intermediate to old age ($t \gtrsim 500\,\mathrm{Myr}$) fractions are similar over the whole spectral region studied. The metallicity has a negligible effect on the propagation of the stellar population fractions derived from NUV to NIR. The same applies to the different EPS models, but restricted to the range between 3800 and 9000 Å. However, a discrepancy between GALEV/Maraston and GRASIL/GALAXEV models occurs in the NIR. Furthermore, the initial mass function is not important for the synthesis propagation. Compared to STARLIGHT synthesis results, our propagation predictions agree at ∼95 per cent confidence level in the optical, and ∼85 per cent in the NIR. In summary, spectral fitting performed in a restricted spectral range should not be directly propagated from the NIR to the UV/optical, or vice versa. We provide equations and an on-line form [panchromatic averaged stellar population (PaASP)] to be used for this purpose.

Key words: stars: AGB and post-AGB – galaxies: star formation – galaxies: stellar content – infrared: general – infrared: stars.

1 INTRODUCTION

A key issue in modern astrophysics is to understand how galaxies form and evolve, and the study of the stellar population and star formation history (over a wide wavelength range) may provide clues to the dominant mechanism. For example, two main scenarios are proposed to explain the formation of galaxies, one is the tidal torque theory, which suggests an initial collapse of gas at very high redshift (e.g. Eggen, Lynden-Bell & Sandage 1962; White 1984), and another is associated with galaxy mergers at intermediate to high redshifts (see e.g. Searle & Zinn 1978; Hammer et al. 2005, 2007, 2009). Both produce distinct signatures in the resulting stellar populations.

As we still cannot access the light of individual stars in almost any galaxy beyond the local group, the way widely used is to study the stellar populations by the integrated light of the whole galaxy or a significant fraction of it, by means of long-slit spectroscopy. The usual approaches for studying unresolved stellar populations are either by means of empirical population synthesis (Bica & Alloin 1987; Bica 1988; Bica et al. 1991; Schmitt, Bica & Pastoriza

1996; Bonatto et al. 1998, 2000; Cid Fernandes, Storchi-Bergmann & Schmitt 1998) or evolutionary population synthesis (EPS) models (Maraston 1998, 2005; Silva et al. 1998; Vazdekis & Arimoto 1999; Bruzual & Charlot 2003; Kotulla et al. 2009), as well as a combination of both techniques (Cid Fernandes et al. 2004, 2005; Riffel et al. 2007, 2008, 2009). By using them, we can infer the age and metallicity distributions of the stellar populations that make up a galaxy's spectral energy distribution (SED).

The study of unresolved stellar populations in galaxies, ranging from star forming to ellipticals, as well as in composite objects and active galaxies, is a common approach in the near-ultraviolet (NUV) and optical bands (Bica 1988; Schmitt et al. 1996; Bonatto et al. 1998, 2000; Cid Fernandes et al. 1998, 2005; González Delgado et al. 1998, 2004; Raimann et al. 2003; Krabbe et al. 2008; Rickes, Pastoriza & Bonatto 2008, 2009). On the other hand, addressing unresolved stellar populations in the near-infrared (NIR) is less common, starting ∼three decades ago (e.g. Rieke et al. 1980), but which seems to be in increasing expansion (Origlia, Moorwood & Oliva 1993; Oliva et al. 1995; Engelbracht et al. 1998; Origlia & Oliva 2000; Lançon et al. 2001; Davies et al. 2006, 2007, 2009; Riffel et al. 2007, 2008, 2009, 2010).

Very recently, Chen et al. (2010) have shown that using different EPS models in the optical leads to different stellar population

⋆E-mail: riffel@ufrgs.br

results. So, it is not reasonable to directly compare stellar populations estimated from different EPS models. They suggest that to get reliable results, one should use the same EPS models to compare different samples. As related issues, can one compare the light fraction results derived, with the same base of elements, in one spectral region to another? Are the population fractions derived in the optical the same in the NUV/NIR? What is the effect of the normalization point used in the synthesis? Does the choice of elements that compose the base [i.e. age, metallicity and initial mass function (IMF)] produce different results along the whole spectrum?

The answer to the above questions would be easy if stellar population synthesis were based on a more physical parameter, like mass fractions. However, given the non-constant stellar mass-to-light (M/L) ratio, mass fractions have a much less direct relation with the observables than light fractions. In this context, we feel motivated to carry out a detailed study of the panchromatic averaged stellar population (PaASP) components over the 3500 Å to 2.5 μm spectral region, commonly used for stellar population synthesis. It should be clear that PaASP is not a tool for performing stellar population synthesis. Instead, it is specifically designed for translating the spectral fitting of galaxies (in terms of light fractions) derived in one spectral domain into another. This paper is structured as follows. The EPS models used are described in Section 2. The methodology and results are presented in Section 3. Results are discussed in Section 4. The final remarks are given in Section 5.

2 THE ADOPTED EPS MODELS

In this section we describe the EPS models used in what follows. The four models, GRASIL, GALEV, Maraston and GALAXEV, have been selected because they have a spectral coverage from the NUV to the NIR region (~3500 Å to 2.5 μm) and are widely used. A brief description of them is made below. Details can be found in the original papers cited below, as well as in Chen et al. (2010).

2.1 GRASIL

The GRAphite and SILicate (GRASIL)[1] code, developed by Silva et al. (1998), is a chemical evolution code that follows the star formation rate, metallicity and gas fraction, which are basic ingredients for stellar population synthesis. The latter is performed with a grid of integrated spectra of simple stellar populations (SSPs) of different ages and metallicities, in which the effects of dusty envelopes around asymptotic giant branch (AGB) stars are included, but not the AGB energetics (Bressan, Granato & Silva 1998; Bressan, Silva & Granato 2002). The models consider four IMFs: Kurucz (1992), Kennicutt et al. (1994), Scalo (1986) and Miller & Scalo (1979). Kurucz (1992) atmosphere models, for population synthesis, and Padova tracks (Bertelli et al. 1994) are also considered. Moreover, SSPs of GRASIL cover a spectral range from 91 Å up to 1200 μm. Further details can be found in Laura Silva PhD thesis.[2]

2.2 GALEV

The GALaxy EVolution (GALEV)[3] evolutionary synthesis models describe the evolution of stellar populations in general, from star clusters to galaxies, both in terms of resolved stellar populations and integrated light properties (Kotulla et al. 2009). According to

the authors, the code considers both the chemical evolution of the gas and the spectral evolution of the stellar component, allowing for a chemically consistent approach. Thus, some SSPs provided by GALEV show an emission-line spectrum.

The SSP models provided by GALEV cover five metallicities and 4000 ages ($0.02 \leq Z/Z_\odot \leq 2.5$ and 4 Myr $\leq t \leq$ 16 Gyr). They are based on the spectra from BaSeL spectral library (Lejeune, Cuisinier & Buser 1997, 1999; Westera et al. 2002), originally based on the Kurucz (1992) library. They also have three different IMFs (Salpeter 1955; Kroupa 2001; Chabrier 2003) and use the theoretical isochrones from the Padova team (e.g. Bertelli et al. 1994; Schulz et al. 2002). The wavelength coverage spans the range from 90 Å to 160 μm, with a spectral resolution of 20 Å in the NUV-optical and 50–100 Å in the NIR. They also include the thermally pulsating asymptotic giant branch (TP-AGB) phase provided by the Padova tracks (Girardi et al. 2002; Schulz et al. 2002). It is also worth mentioning at this point that the TP-AGB stars account for 25 to 40 per cent of the bolometric light of an SSP, and for 40 to 60 per cent of the light emitted in the K band (e.g. Schulz et al. 2002; Maraston 2005, and references therein). In addition, contrary to (Maraston 2005) (see below), GALEV models do not include empirical TP-AGB spectra. For a detailed description of GALEV, see Kotulla et al. (2009).

2.3 Maraston models

The Maraston EPS models[4] (hereafter M05) are being developed by Claudia Maraston since 1998 (Maraston 1998) with an update in 2005 (Maraston 2005). They are based on the fuel consumption theorem and include a proper treatment of the TP-AGB phase. According to these models, the effects of TP-AGB stars in the NIR spectra are unavoidable. The M05 models, by including empirical spectra of oxygen- and carbon-rich stars (Lançon & Wood 2000), can predict the presence of NIR absorption features such as the 1.1 μm CN band (Riffel et al. 2007, 2008, 2009), whose detection can be taken as an unambiguous evidence of a young- to intermediate-age stellar population. The models have been used by our team to study stellar populations in active galactic nuclei and starburst galaxies (see Riffel et al. 2007, 2008, 2009, 2010 for CN, see also Dottori et al. 2005; Ramos-Almeida et al. 2008) as well as in the age dating of massive galaxies at high redshift (Maraston et al. 2006; van der Wel et al. 2006; Rodighiero et al. 2007; Cimatti et al. 2008).

M05 models span a range of six different metallicities ($1/200 \leq Z/Z_\odot \leq 3.5$) with ages distributed from 1 Myr to 15 Gyr according to a grid of 67 models (Note that the full age grid is not available for all metallicities, M05.) The IMFs considered are Salpeter (1955) and Kroupa (2001). The stellar spectra were also taken from the BaSel library. The spectral range is from 91 Å to 160 μm, with a spectral resolution of 5–10 Å up to the optical region, and 20–100 Å in the NIR. In Maraston (1998, 2005) models, the TP-AGB contributes 40 per cent to the bolometric flux, but rising to 80 per cent when only the K band is considered.

2.4 GALAXEV

GALAXEV[5] is a widely used library of evolutionary stellar population synthesis models. It is computed with the isochrones

---

[1] Available at http://adlibitum.oats.inaf.it/silva/grasil/grasil.html
[2] see: http://adlibitum.oats.inaf.it/silva/laura/laura.html
[3] http://www.galev.org

[4] Available at http://www-astro.physics.ox.ac.uk/~maraston/
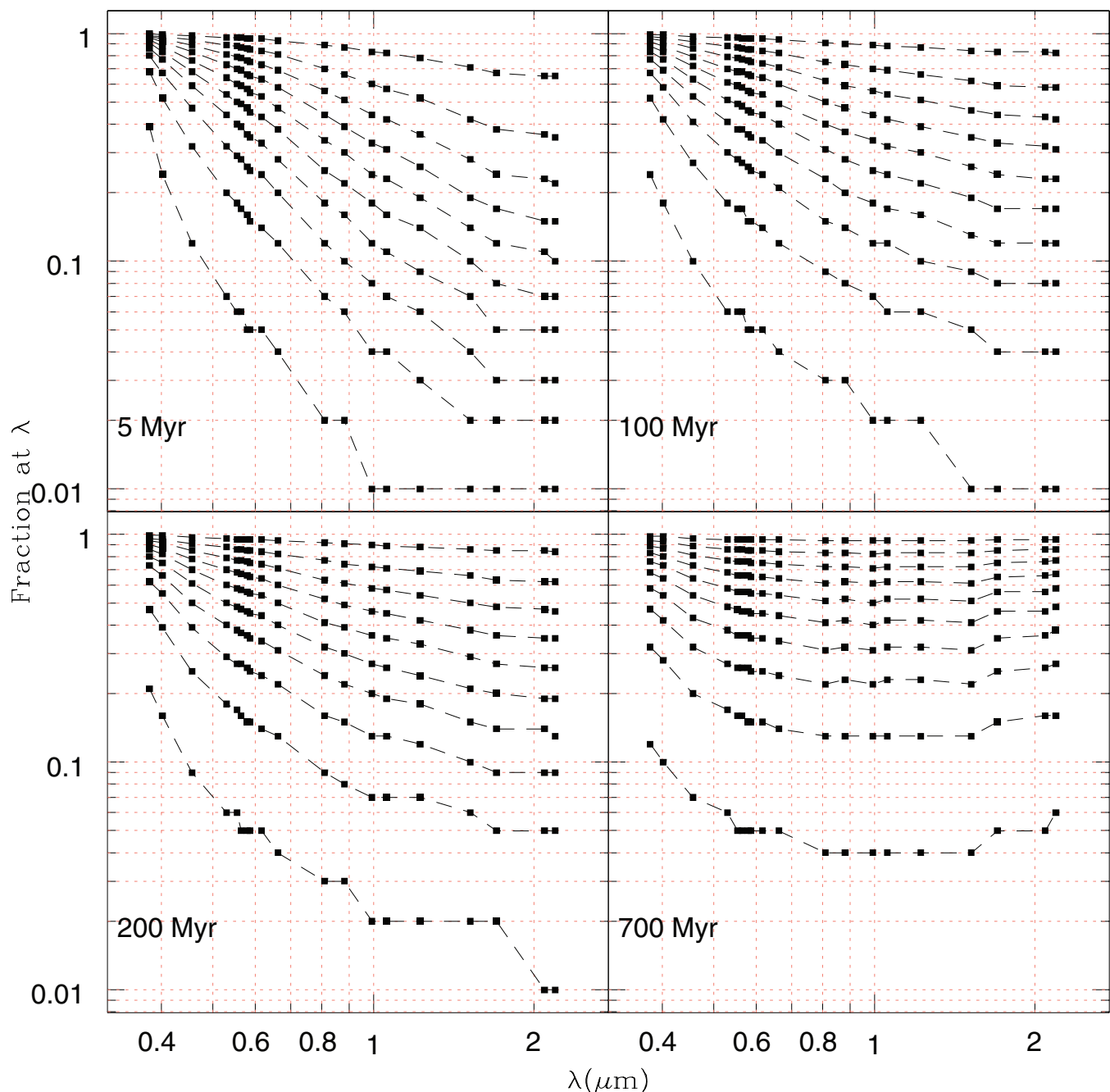[5] Available at http://www.cida.ve/~bruzual/bc2003

Figure 1. Light fraction at λ for the stellar population components. The curves result from equation (2) with increasing fractions of 10 per cent of the 'young' component from bottom to top. In each panel we start with 5 per cent of the flux of the 'young' SSP+95 per cent of the 13 Gyr SSP, and finish with 95 per cent of the young+5 per cent of the old component. The ages of the 'young' component are on the labels. The normalization point for the combination was 5870 Å. We use the M05 models as reference. See text for more details.

synthesis code of Bruzual & Charlot (2003, also known as BC03). The spectral coverage of this library is from 91 Å up to 160 µm, with a resolution of 3 Å between 3200 and 9500 Å, and a lower resolution elsewhere. Ages range from 1×10^5 up to 2×10^{10} yr, for a wide range of metallicities ($1/200 \lesssim Z/Z_\odot \lesssim 2.5$). These models use the STELIB/BaSeL libraries (see Lejeune et al. 1997, 1999; Westera et al. 2002, and references therein) as well as the STELIB/Pickles libraries (Pickles 1998). GALAXEV allows the use of two IMFs (Salpeter 1955; Chabrier 2003) and three stellar evolution tracks: Geneva (Schaller et al. 1992), Padova 94 (Alongi et al. 1993;

Bressan et al. 1993; Fagotto et al. 1994a,b; Girardi et al. 1996) and Padova 00 (Girardi et al. 2000). These models do not include the TP-AGB phase.

3 METHODOLOGY AND RESULTS

First, we investigate the dependence of the stellar population components on the normalization point, from the NUV to the NIR. To do this, we select spectral regions free from emission/absorption lines

to be used as normalization points, F_λ. They are 3800, 4020, 4570, 5300, 5545, 5650, 5800, 5870, 6170, 6620, 8100, 8815, 9940 Å, 1.058, 1.223, 1.520, 1.701, 2.092 and 2.19 μm (Bica 1988; Saraiva et al. 2001; Cid Fernandes et al. 2004; Rickes et al. 2008, 2009; Riffel et al. 2008).

In addition, we select SSPs with ages 0.005, 0.025, 0.050, 0.1, 0.2, 0.3, 0.4 0.5, 0.6, 0.7, 0.8, 0.9, 1.0, 2.0, 5.0 and 13 Gyr as representative of the stellar populations observed in galaxies. As a first exercise we combine two components: 13 Gry (the old population) and one of the other SSPs representing the 'young' population. The combination was made by summing up, along the whole spectral range (∼3500 Å to 2.5 μm), increasing fractions of the 'young' component from 1 to 100 per cent,

according to

$$F = (1 - f)\,F_y + f\,F_o, \tag{1}$$

where f is the fractional flux, which we vary in steps of 0.01, F_y is the flux of spectrum of the 'young' component, for each λ between ∼3500 Å and 2.5 μm, normalized to unity at 5870 Å for the optical, or at 1.223 μm for the NIR, and F_o is the flux of the 13 Gyr spectrum also normalized at the same points. Note that the normalization of the spectra is done by dividing their fluxes by that of the normalization point (5870 Å or 1.223 μm), after the computations are done. In addition, by normalizing the spectra we are dealing with light fractions, which are directly related to the observations. F is the resulting flux of the combined SSPs (young+old) at a specific λ.
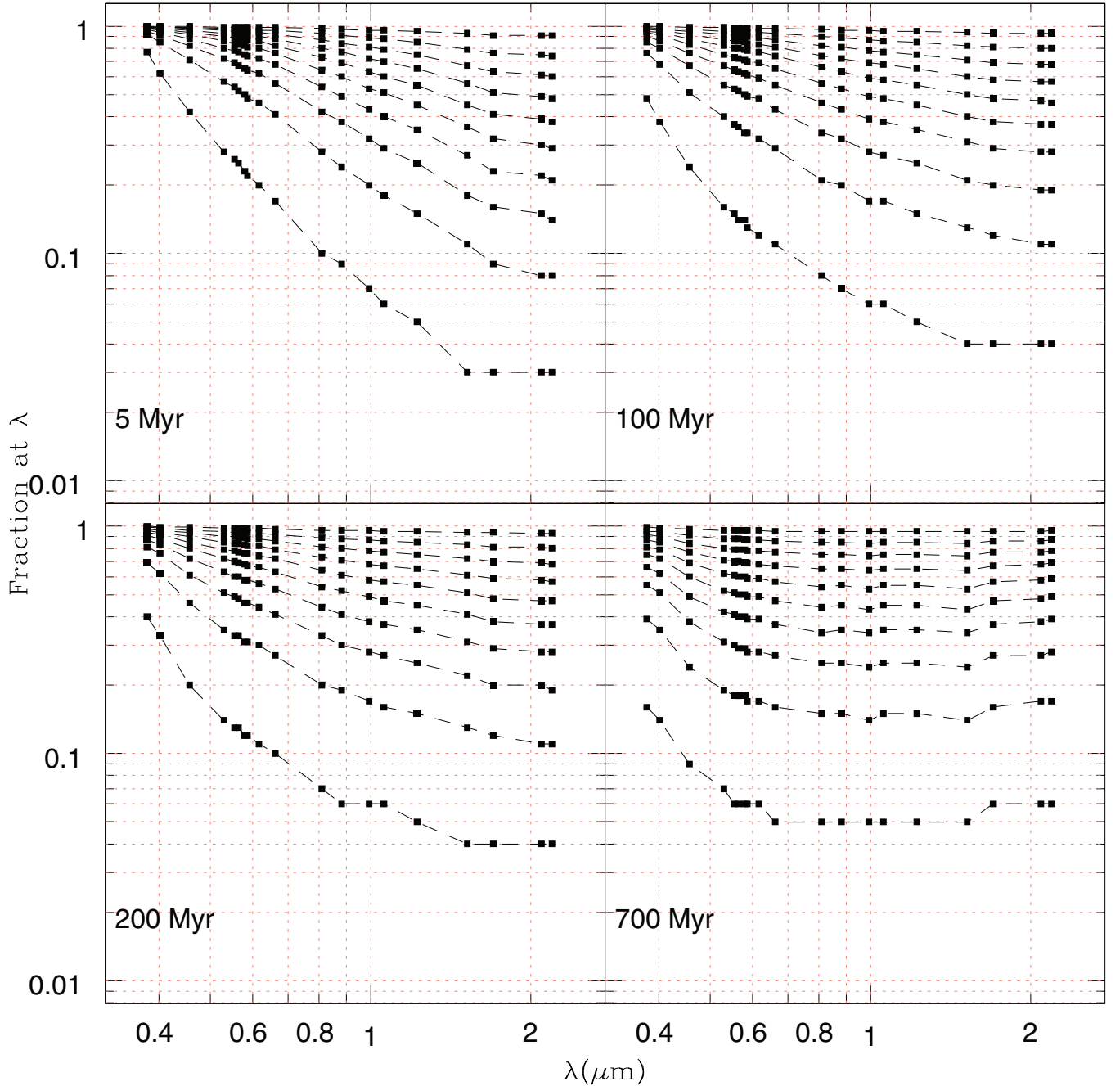

Figure 2. Same as Fig. 1 but for the normalization point at 1.223 μm.

The averaged stellar population components spread over all F_λ were derived by

$$f_y = \frac{(1-f)F_y}{F} \quad \text{and} \quad f_o = \frac{f F_o}{F}. \tag{2}$$

Equation (2) represents the young and old light fractions for different F_λ, this is what we call fraction at λ. The result of such process is summarized in Figs 1 and 2. In these figures we show the sum of a 'young' component with a 13 Gyr SSP (the old component) in steps of 10 per cent. In practice we start with 5 per cent of the flux of the 'young' SSP+95 per cent of the flux of the 13 Gyr SSP, and finish with 95 per cent of the young+5 per cent of the old component. This procedure is done over all λs between the NUV and NIR. It is worth mentioning that Figs 1 and 2 show M05 EPS models as reference (Section 4). These figures suggest that one cannot directly compare the light fractions of the young component ($t \lesssim 400$ Myr) derived in the optical with those obtained in the NIR, and vice versa (i.e. 77 per cent of the 5-Myr population at 3800 Å represents only 5 per cent at 1.223 µm). However, the intermediate to old components ($t \gtrsim 500$ Myr) can be directly compared between different wavelengths. This does not occur when dealing with mass fractions, since the age derived by the mass fraction is a more physical parameter, but has a much less direct relation with the observables, depending strongly on the M/L ratio, which is not constant. Thus, the light fraction can be taken as a direct observable parameter and use equations (1) and (2) to propagate the results over other spectral regions (see Appendix A).

However, the stellar population of galaxies is not so simple as two components. Therefore, we have divided our SSPs into three population vectors $x_y = 0.005$ Gyr, $x_i = 0.025$–1.0 Gyr and $x_o =$

13 Gyr. To investigate the effect of adding one more component to the above exercise, we combined three population vectors according to

$$F' = \frac{1}{100}(\gamma F_y + \delta F_i + \eta F_o)$$
$$\text{with} \quad \gamma + \delta + \eta = 100, \tag{3}$$

where γ, δ and η are the fractional fluxes from 0 to 100 per cent, which are varied in steps of 1 per cent; F_y, F_i and F_o are the normalized fluxes (at $\lambda = 5870$ Å or $\lambda = 1.223$ µm) of the x_y, x_i and x_o population vectors, respectively. F' is the resulting flux of the combined SSPs (young+intermediate+old) at a specific λ.

The averaged stellar population components distributed over all λs were derived similarly to equation (2):

$$f'_y = \frac{\gamma F_y}{F'}, \quad f'_i = \frac{\delta F_i}{F'} \quad \text{and} \quad f'_o = \frac{\eta F_o}{F'}. \tag{4}$$

We show the result of such combination in Figs 3–5. It is clear that even with three population vectors, the results derived in one wavelength are not the same as in other λs. In addition, Fig. 5 reinforces the fact that in the case of only intermediate to old components, the population fractions derived in one wavelength are nearly the same as in other λs (i.e. the values derived in the optical can be used in the NIR).

4 DISCUSSION

The determination of mean ages and metallicities of galaxies is important for models of galaxy formation and evolution. The techniques for dating unresolved stellar populations in local galaxies
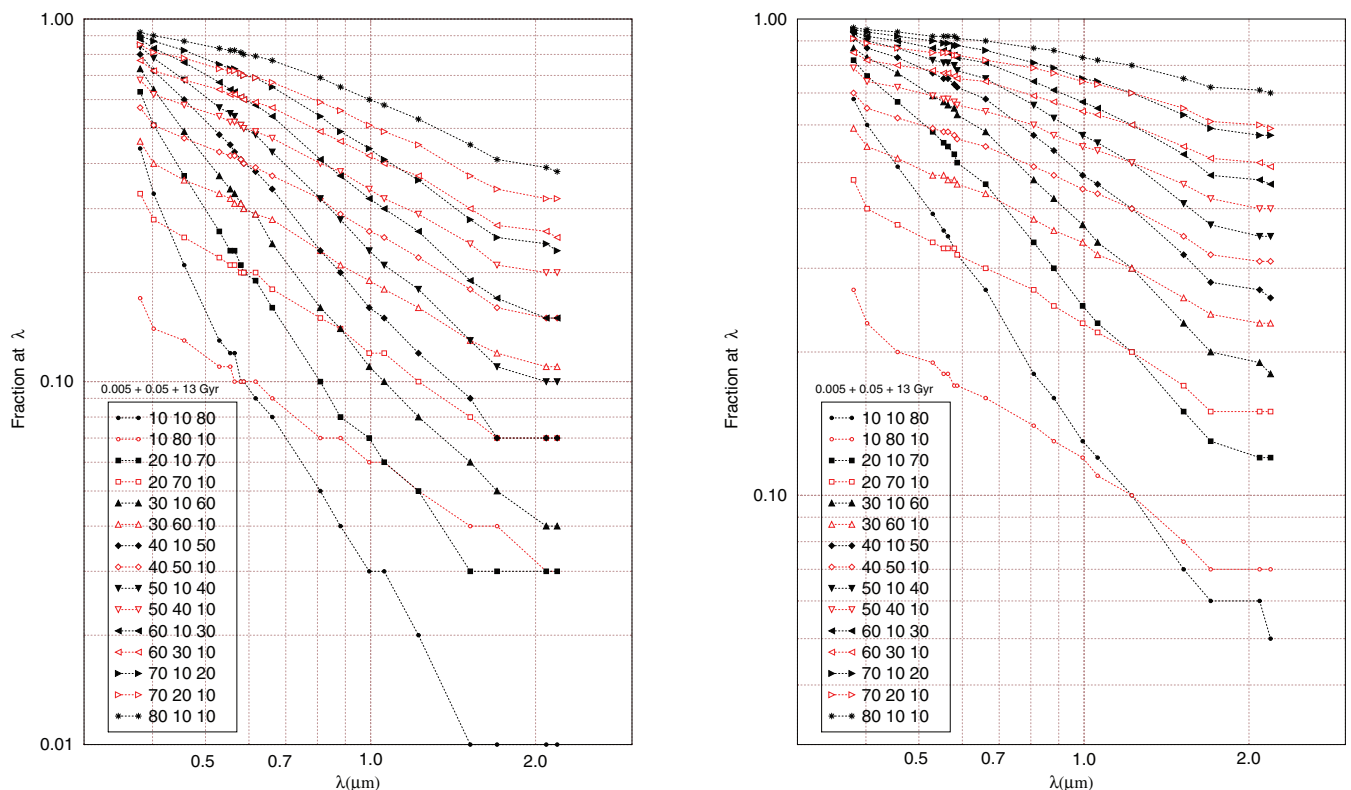

Figure 3. Light fraction at λ for the stellar population components. The curves result from equation (4) with increasing fractions from bottom to top in each panel. The ages and the percentage fluxes are on the labels. The 5-Myr fraction increases from bottom to top. The normalization points are 5870 Å (left-hand panel) and 1.223 µm (right-hand panel). We use the M05 models as reference.
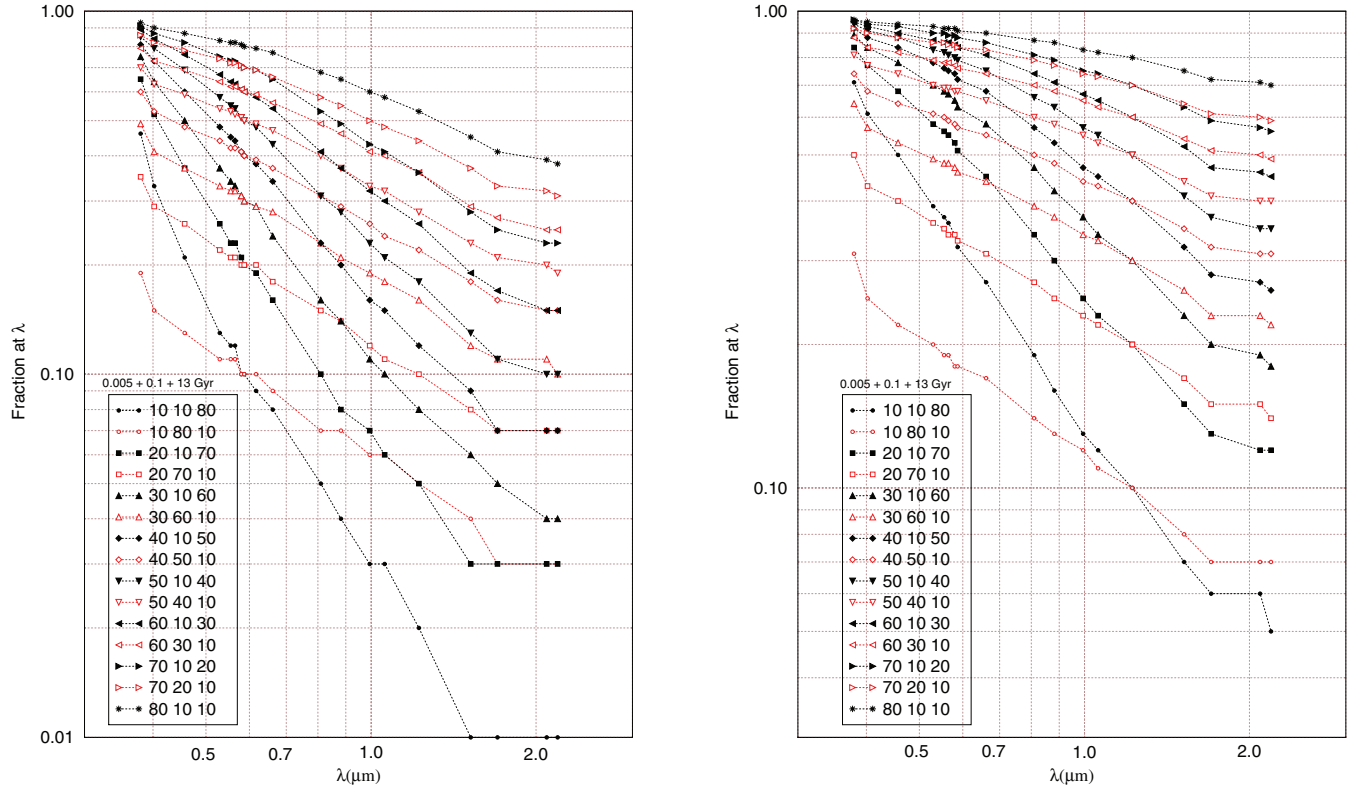
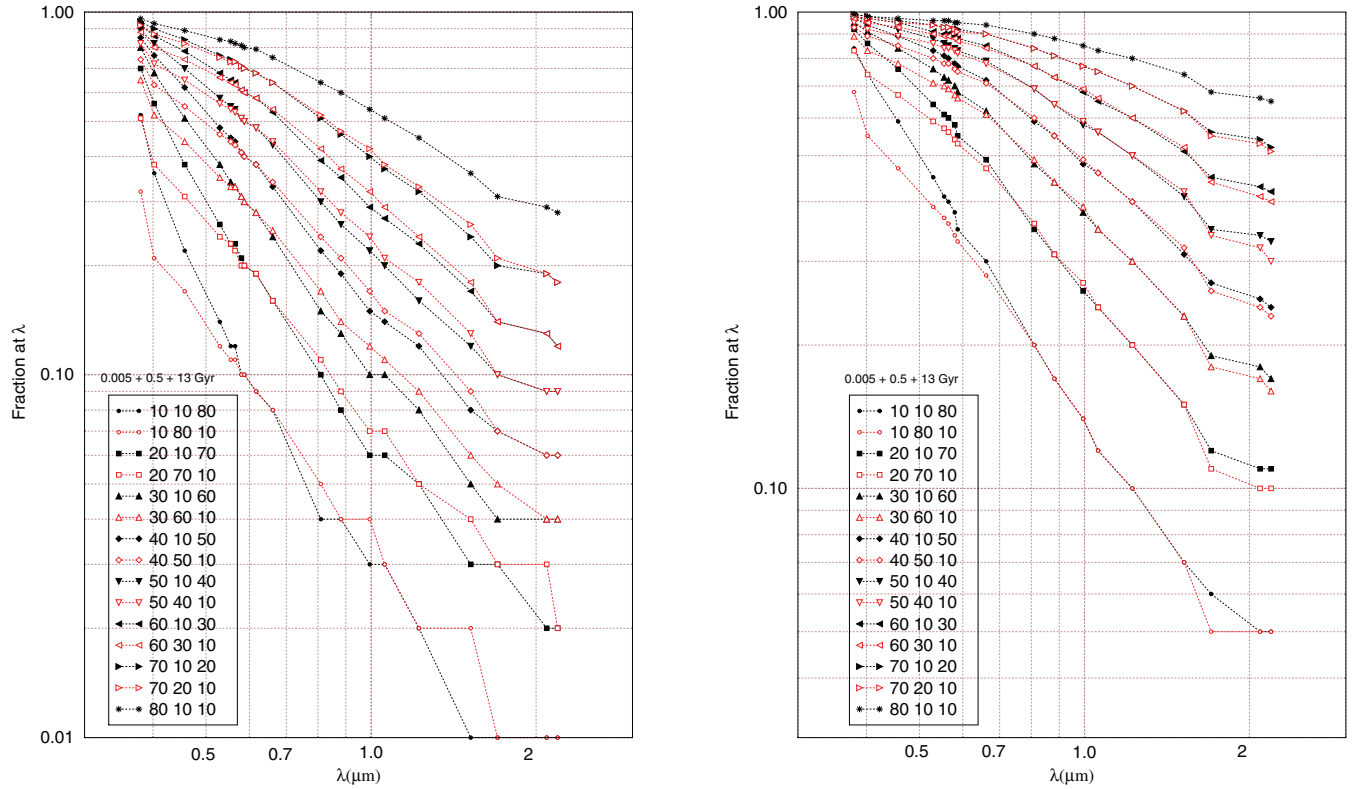**Figure 4.** Same as Fig. 3 but for a different set of ages.

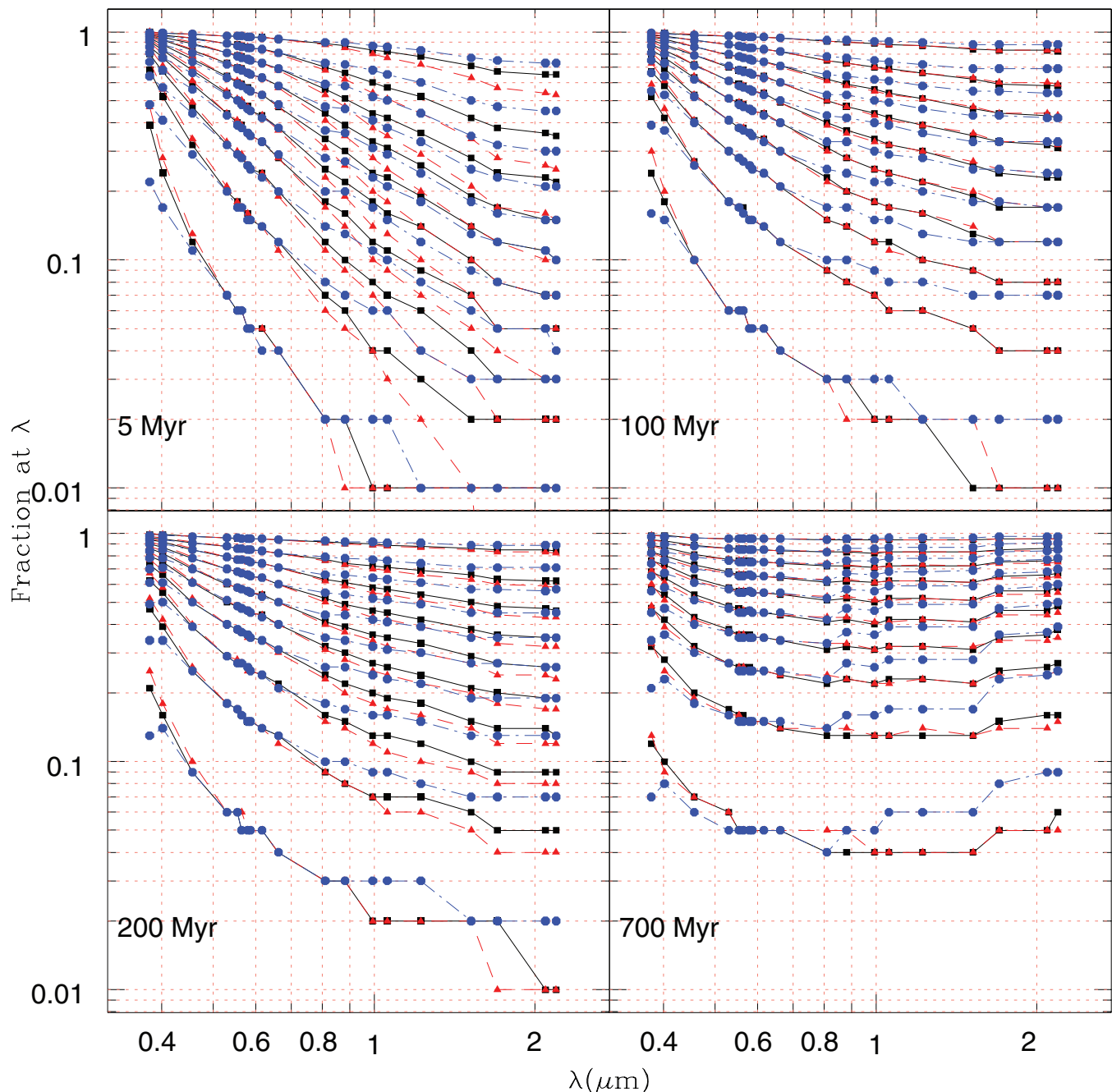**Figure 5.** Same as Fig. 3 but for a different set of ages.

Figure 6. Metallicity effect for the normalization point at 5870 Å. Boxes represent solar metallicity, circles $1/50 \, Z_\odot$ and triangles are $2 \, Z_\odot$. We use the M05 models as reference.

have focused on colours or spectroscopic indices measured in the NUV and optical (e.g. Bica 1988; Worthey 1994; Bica et al. 1996; Bonatto et al. 1996, 1998; Maraston & Thomas 2000; Trager et al. 2000a,b; Thomas et al. 2005, and references therein). However, even small mass fractions of young stars added to an old population can affect the NUV and optical age determinations significantly, making the galaxy appear young, which leads to a further degeneracy between mass fraction and age (Thomas & Davies 2006; Serra & Trager 2007). These problems may be solved for intermediate-age stellar populations looking in NIR wavelengths. In addition, the detection of young stellar populations in the NIR requires a hard work (Riffel et al. 2010). Nevertheless, it is clear from Fig. 2 that even a small fraction of a 5-Myr population (∼5 per cent) detected

in the NIR may be responsible for almost all the light observed in the NUV (∼70 per cent).

Clearly, synthesis results should not be directly propagated from the NIR to the NUV/optical, or vice versa. Instead, equations (2)–(4) should be used for this purpose. To help with such a comparison we have created an on-line form the PaASP[6] and make available for download the tables with the results of the above equations (see Appendix A).

Another important ingredient in stellar population fitting is the metallicities used. As shown by Chen et al. (2010), the results of the
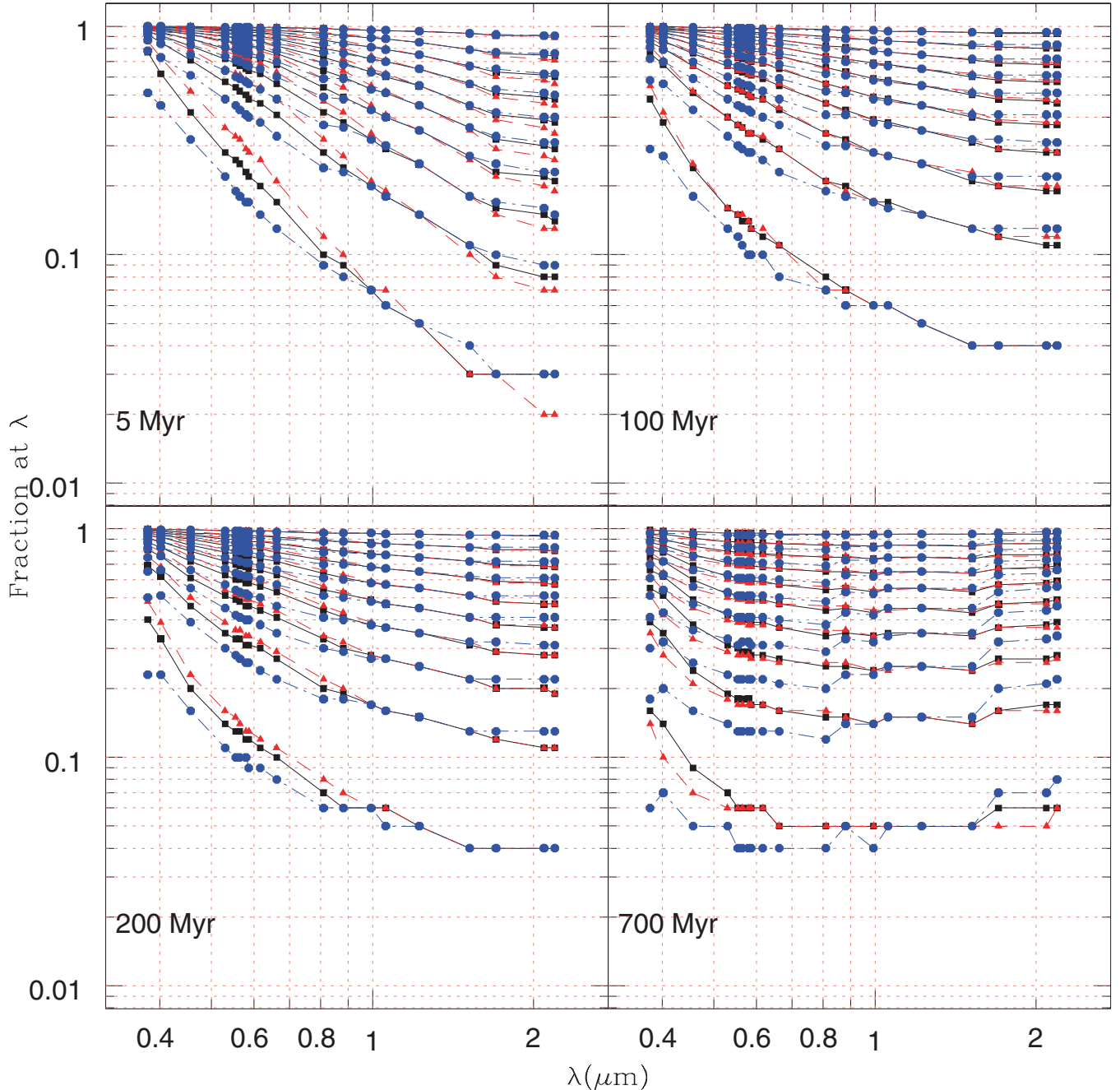
[6] Available at http://www.if.ufrgs.br/~riffel/software.html

Figure 7. Same as Fig. 6 but for the normalization point at 1.223 µm.

fitting have a weaker dependence on metallicity than age. The question that arises here is, does metallicity affect the propagation of the averaged stellar populations? We investigate this effect with M05 SSPs with three different metallicities ($1/50\,Z_\odot$, $Z_\odot$ and $2\,Z_\odot$) and the same age grid as in Fig. 1. The results are shown in Figs 6 and 7. Clearly the propagation of the contributions has a negligible dependence on metallicity. Thus, one can use the condensed population vectors proposed by Cid Fernandes et al. (2004, 2005) to propagate the fitting results over all λs.

All the tests described above were made using the M05 models, but, as stated in Section 2, there are more EPS models available in the literature covering simultaneously the spectral region between ~3500 Å and 2.5 µm. Thus, it is necessary to test if the selection

of EPS models will produce different results in the propagation of the synthesis results over different λs. In Fig. 8 we compare the different models among each other. It is clear that in the case of the optical normalization point (5870 Å), the four models produce very similar results in the interval between 3800 and 9000 Å, but a discrepancy between GALEV/M05 and GRASIL/BC03 models is observed in the NIR. Such a discrepancy is due to the well known fact that GALEV and M05 models do include stars in the TP-AGB phase (see e.g. M05), which is more sensitive to the NIR than the optical, i.e. TP-AGB stars account for 25 to 40 per cent of the bolometric light of an SSP, and for 40 to 60 per cent of the light emitted in the *K* band (see Schulz et al. 2002; Maraston 2005, and references therein). However, there is a difference between GALEV
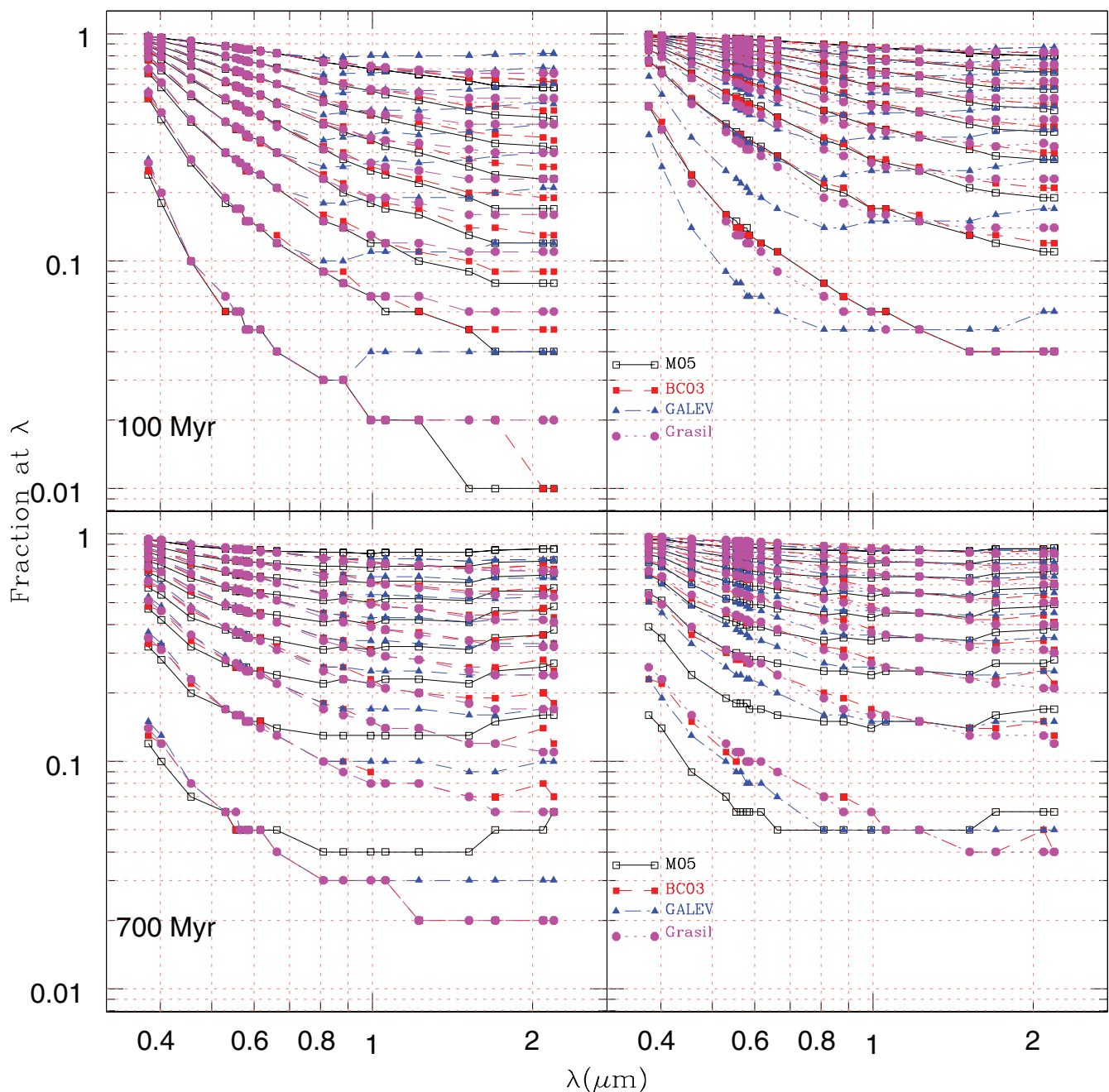
Figure 8. Comparison of different EPS models. Normalized at 5870 Å (left) and 1.223 μm (right). Note that we use 100 Myr+13 Gyr SSPs.

and M05 models, enhanced in the 100-Myr population. There are two possible explanations for this discrepancy: one is associated with the different onset age of the TP-AGB on the models. A high TP-AGB contribution at 100 Myr, as applied by Schulz et al. (2002), which is excessively high when compared to young Large Magellanic Cloud globular clusters (Maraston 1998; Marigo et al. 2008). The other is associated with the way in which the TP-AGB treatment is made (Maraston et al. 2006; Bruzual 2007). GALEV includes TP-AGB by means of isochrones (Padova94+improved TP-AGB models; Bertelli et al. 1994; Girardi et al. 2000; Marigo et al. 2008), while M05 is based on a different approach, the fuel consumption theorem. According to Maraston (2005), the stellar luminosity during the evolutionary phases that follow or suffer from mass loss cannot be predicted by stellar tracks, because there is no

theory linking mass-loss rates to the basic stellar parameters, such as luminosity.

Note that the trend observed in Fig. 8 can also be associated with the fact that in M05 models, the TP-AGB contributes with 40 per cent to the bolometric flux, and 80 per cent to the K band. This is higher than the 'simpler' calculations (made by the Padova group at the time) used by Schulz et al. (2002), in which only some thermal pulses have been included (Girardi et al. 2000).

In addition, the tests were performed with the Salpeter (1955) IMF. To see the effect of the IMF on the averaged stellar populations over all λs, we repeat the same exercises for different IMFs and summarize the results in Fig. 9. This figure suggests that the IMF does not play an important role in the synthesis propagation to other spectral regions.
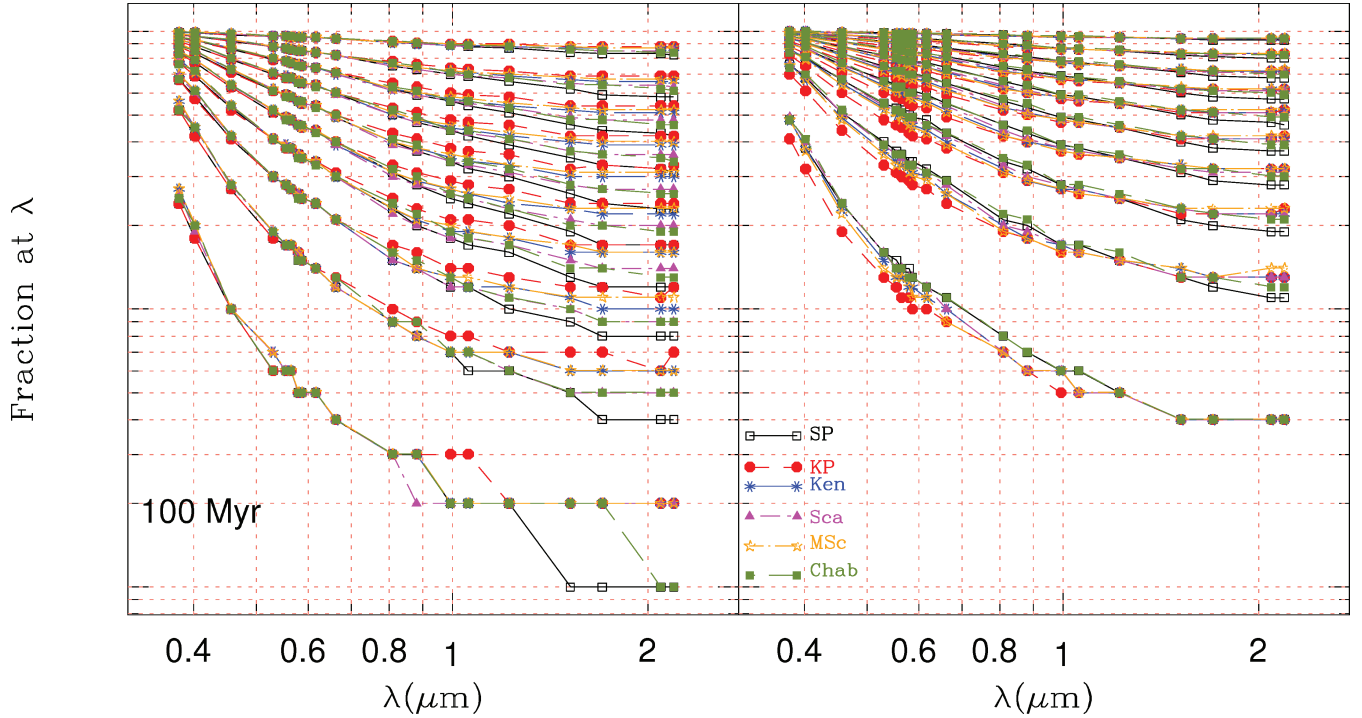
Figure 9. Effect of different IMFs. At left the normalization point is 5870 Å and at right 1.223 μm. Salpeter (SP) and Kroupa (KP) were taken from M05 models; Kennicutt (Ken), Scalo (Sca) and Miller & Scalo (MSc) IMFs were taken from GRASIL EPS and Chabrier (Chab) was taken from GALAXEV.

4.1 Testing PaASP

In order to test if we are able to predict the averaged stellar populations over all λs, extensive simulations were performed to evaluate the PaASP's ability to recover input parameters. In short, we build artificial galaxy spectra by mixing Maraston (2005) solar metallicity SSP models of 5 Myr, 700 Myr and 13 Gyr in different proportions, and perform stellar population synthesis with normalization points at the optical (5870 Å) and NIR (12 230 Å). To this purpose we use the STARLIGHT code optimized to the optical region (Cid Fernandes et al. 2004, 2005, 2009; Mateus et al. 2006; Asari et al. 2007), and which also produces reliable results when applied to the NIR spectra (Riffel et al. 2009, 2010).

In summary, STARLIGHT fits an observed spectrum O_λ with a combination, in different proportions, of N_* SSPs. Basically, it solves the following equation (Cid Fernandes et al. 2005):

$$M_\lambda = M_{\lambda 0} \left[\sum_{j=1}^{N_*} x_j \, b_{j,\lambda} \, r_\lambda \right] \otimes G(v_*, \sigma_*), \qquad (5)$$

where M_λ is a model spectrum, $b_{j,\lambda} r_\lambda$ is the reddened spectrum of the jth SSP normalized at λ_0, $r_\lambda = 10^{-0.4(A_\lambda - A_{\lambda 0})}$ is the reddening term, $M_{\lambda 0}$ is the synthetic flux at the normalization wavelength, $\boldsymbol{x}$ is the population vector, $\otimes$ denotes the convolution operator and $G(v_*, \sigma_*)$ is the Gaussian distribution used to model the line-of-sight stellar motions, which is centred at velocity v_* with dispersion σ_*. The final fit is carried out with a simulated annealing plus Metropolis scheme, which searches for the minimum of the equation:

$$\chi^2 = \sum_\lambda [(O_\lambda - M_\lambda) w_\lambda]^2, \qquad (6)$$

where emission lines and spurious features are masked out by fixing $w_\lambda = 0$. For a detailed description of STARLIGHT see Cid Fernandes et al. (2004, 2005).

As base set we take Maraston (2005) SSPs covering 14 ages, $t =$ 0.001, 0.005, 0.01, 0.03, 0.05, 0.1, 0.2, 0.5, 0.7, 1, 2, 5, 9, 13 Gyr, and four metallicities, namely: $Z = 0.02, 0.5, 1$ and $2\,Z_\odot$, summing up 56 elements.

To compare STARLIGHT with PaASP predictions, we use the condensed population vector, which is obtained by binning the synthesis results into young, x_Y ($t \leq 5 \times 10^7$ yr); intermediate, x_I ($1 \times 10^8 \leq t \leq 2 \times 10^9$ yr) and old, x_O ($t > 2 \times 10^9$ yr) components (Cid Fernandes et al. 2004; Riffel et al. 2009). These components were then taken to represent the 5 Myr, 700 Myr and 13 Gyr old populations. These vectors are compared with the PaASP predictions in Fig. 10.

Clearly, our predictions are consistent with the stellar population synthesis, especially at the optical region, where the confidence level between predictions and synthesis is ~95 per cent (i.e. almost all points fall in a region less than 5 per cent from the identity line). The confidence level drops to ~85 per cent in the NIR.

5 FINAL REMARKS

We study the panchromatic stellar population components over the 3500 Å to 2.5 μm spectral region. In particular, we analyse how the spectral fitting of galaxies based on light fractions derived in a given spectral range can be propagated over all λs. Dependencies on EPS models, age, metallicity and stellar evolution tracks of four widely used EPS models (GRASIL, GALEV, Maraston and GALAXEV) were taken into account. Our main results are as follows.

(i) The young ($t \lesssim 400$ Myr) stellar population fractions derived in the optical cannot be directly compared to those derived in the NIR, and vice versa. For example, a contribution of ~80 per cent of a 5-Myr population at 3800 Å translates into only 5 per cent at 1.223 μm.
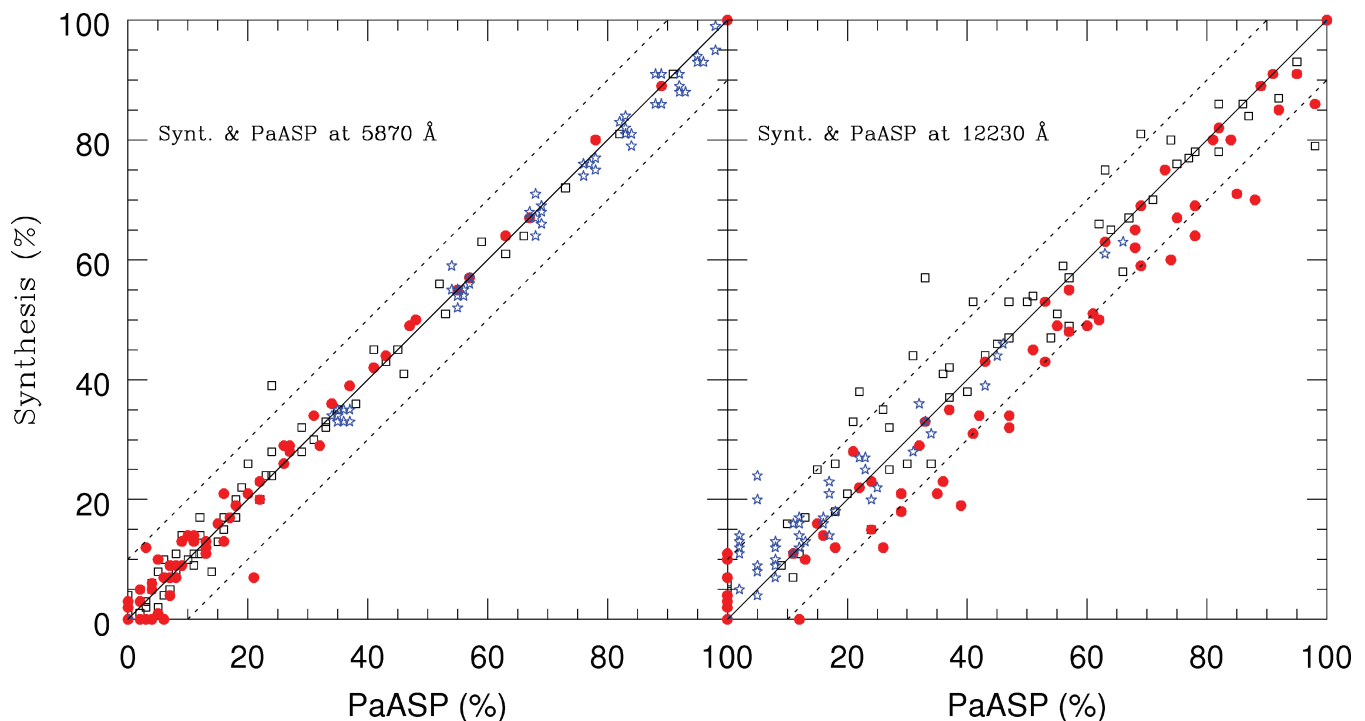
Figure 10. PaASP tests. Stars, boxes and circles represent the 5 Myr, 700 Myr and 13 Gyr SSPs, respectively. Identity is shown by the solid line and dotted lines indicate the 90 per cent confidence level.

(ii) The intermediate- to old-age components ($t \gtrsim 500\,\text{Myr}$) can be directly compared from the NUV up to the NIR.

(iii) The metallicity dependence on the propagation of the stellar population fractions derived from NUV to NIR is negligible.

(iv) Different EPS models produce similar results in the propagation of the synthesis results over the interval between 3800 and 9000 Å. However, a discrepancy between GALEV/M05 and GRASIL/BC03 models occurs in the NIR. Such a discrepancy may be due to the fact that GALEV and M05 models do include stars in the TP-AGB phase.

(v) There is a difference between GALEV and M05 models, enhanced in the 100-Myr population. Such a discrepancy may be associated with the way in which the TP-AGB treatment is made (Maraston et al. 2006; Bruzual 2007).

(vi) We test the effect of six different IMFs, and we conclude that the IMF is not important in the propagation of the synthesis results.

(vii) Extensive simulations were performed to evaluate PaASP's ability to recover input parameters. Our predictions are consistent with the stellar population synthesis with a confidence level between the predictions and synthesis of ∼95 per cent in the optical and ∼85 per cent in the NIR.

In summary, spectral fitting results should not be directly propagated from the NIR to the NUV/optical, or vice versa. Instead, equations (2)–(4) should be used for this purpose. However, since this is hard to do when dealing with large samples of objects, we have created an on-line form, the PaASP, available at http://www.if.ufrgs.br/∼riffel/software.html. We also make available for download the tables with the results of the above equations for a wide range of ages (see Appendix A).

ACKNOWLEDGMENTS

REFERENCES

Alongi M., Bertelli G., Bressan A., Chiosi C., Fagotto F., 1993, A&AS, 97, 851

Asari N. V., Cid Fernandes R., Stasińska G., Torres-Papaqui J. P., Mateus A., Sodré L., Schoenell W., Gomes J. M., 2007, MNRAS, 381, 263

Bertelli G., Bressan A., Chiosi C., Fagotto F., Nasi E., 1994, A&AS, 106, 275

Bica E., 1988, A&A, 195, 9

Bica E., Alloin D., 1987, A&A, 186, 49

Bica E., Pastoriza M. G., da Silva L. A. L., Dottori H., Maia M., 1991, AJ, 102, 1702

Bica E., Bonatto C., Pastoriza M. G., Alloin D., 1996, A&A, 313, 405

Bonatto C., Bica E., Pastoriza M. G., Alloin D., 1996, A&AS, 118, 89

Bonatto C., Pastoriza M. G., Alloin D., Bica E., 1998, A&A, 334, 439

Bonatto C., Bica E., Pastoriza M. G., Alloin D., 2000, A&A, 355, 99

Bressan A., Fagotto F., Bertelli G., Chiosi C., 1993, A&AS, 100, 647

Bressan A., Granato G. L., Silva L., 1998, A&A, 332, 135

Bressan A., Silva L., Granato G. L., 2002, A&A, 392, 377

Bruzual G., 2007, in Vallenari A., Tantalo R., Portinari L., Moretti A., eds, ASP Conf. Ser. Vol. 374, From Stars to Galaxies: Building the Pieces to Build Up the Universe. Astron. Soc. Pac., San Francisco, p. 303

Bruzual G., Charlot S., 2003, MNRAS, 344, 1000

Chabrier G., 2003, PASP, 115, 763

Chen X. Y., Liang Y. C., Hammer F., Prugniel P., Zhong G. H., Rodrigues M., Zhao Y. H., Flores H., 2010, A&A, 515, 101

Cid Fernandes R., Jr, Storchi-Bergmann T., Schmitt H. R., 1998, MNRAS, 297, 579

Cid Fernandes R., Gu Q., Melnick J., Terlevich E., Terlevich R., Kunth D., Rodrigues Lacerda R., Joguet B., 2004, MNRAS, 355, 273

Cid Fernandes R., Mateus A., Sodré L., Stasińska G., Gomes J. M., 2005, MNRAS, 358, 363

Cid Fernandes R. et al., 2009, Rev. Mex. Astron. Astrofís. Conf. Ser., 35, 127

Cimatti A. et al., 2008, A&A, 482, 21

Davies R. I. et al., 2006, ApJ, 646, 754

Davies R. I., Mueller Sánchez F., Genzel R., Tacconi L. J., Hicks E. K. S., Friedrich S., Sternberg A., 2007, ApJ, 671, 1388

Davies R., Maciejewski W., Hicks E., Tacconi L., Genzel R., Engel H., 2009, ApJ, 702, 114

Dottori H., Díaz R. J., Carranza G., Lípari S., Santos J., Jr, 2005, ApJ, 628, L85

Eggen O. J., Lynden-Bell D., Sandage A. R., 1962, ApJ, 136, 748

Engelbracht C. W., Rieke M. J., Rieke G. H., Kelly D. M., Achtermann J. M., 1998, ApJ, 505, 639

Fagotto F., Bressan A., Bertelli G., Chiosi C., 1994a, A&AS, 104, 365

Fagotto F., Bressan A., Bertelli G., Chiosi C., 1994b, A&AS, 105, 29

Girardi L., Bressan A., Chiosi C., Bertelli G., Nasi E., 1996, A&AS, 117, 113

Girardi L., Bressan A., Bertelli G., Chiosi C., 2000, A&AS, 141, 371

Girardi L., Bressan A., Bertelli G., Chiosi C., 2002, A&AS, 141, 371

González Delgado R. M., Leitherer C., Heckman T., Lowenthal J. D., Ferguson H. C., Robert C., 1998, ApJ, 495, 698

González Delgado R. M., Cid Fernandes R., Pèrez E., Martins L. P., Storchi-Bergmann T., Schmitt H., Heckman T., Leitherer C., 2004, ApJ, 605, 127

Hammer F., Flores H., Elbaz D., Zheng X. Z., Liang Y. C., Cesarsky C., 2005, A&A, 430, 115

Hammer F., Puech M., Chemin L., Flores H., Lehnert M. D., 2007, ApJ, 662, 322

Hammer F., Flores H., Puech M., Yang Y. B., Athanassoula E., Rodrigues M., Delgado R., 2009, A&A, 507, 1313

Kennicutt R. C., Jr, Tamblyn P., Congdon C. E., 1994, ApJ, 435, 22

Kotulla R., Fritze U., Weilbacher P., Anders P., 2009, MNRAS, 396, 462

Krabbe A. C., Pastoriza M. G., Winge C., Rodrigues I., Ferreiro D. L., 2008, MNRAS, 389, 1593

Kroupa P., 2001, MNRAS, 322, 231

Kurucz R. L., 1992, in Barbuy B., Renzini A., eds, Proc. IAU Symp. Vol. 149, The Stellar Populations of Galaxies. Kluwer, Dordrecht, p. 225

Lançon A., Wood P. R., 2000, A&AS, 146, 217

Lançon A., Goldader J. D., Leitherer C., González Delgado R. M., 2001, ApJ, 552, 150

Lejeune Th., Cuisinier F., Buser R., 1997, A&AS, 125, 229

Lejeune Th., Cuisinier F., Buser R., 1998, A&AS, 130, 65

Maraston C., 1998, MNRAS, 300, 872

Maraston C., 2005, MNRAS, 362, 799

Maraston C., Thomas D., 2000, ApJ, 541, 126

Maraston C., Daddi E., Renzini A., Cimatti A., Dickinson M., Papovich C., Pasquali A., Pirzkal N., 2006, ApJ, 652, 85

Marigo P., Girardi L., Bressan A., Groenewegen M. A. T., Silva L., Granato G. L., 2008, A&A, 482, 883

Mateus A., Sodré L., Cid Fernandes R., Stasińska G., Schoenell W., Gomes J. M., 2006, MNRAS, 370, 721

Miller G. E., Scalo J. M., 1979, ApJS, 41, 513

Oliva E., Origlia L., Kotilainen J. K., Moorwood A. F. M., 1995, A&A, 301, 55

Origlia L., Oliva E., 2000, New Astron. Rev., 44, 257

Origlia L., Moorwood A. F. M., Oliva E., 1993, A&A, 280, 536

Pickles A. J., 1998, PASP, 110, 863

Raimann D., Storchi-Bergmann T., González Delgado R. M., Cid Fernandes R., Heckman T., Leitherer C., Schmitt H., 2003, MNRAS, 339, 772

Ramos A. C., Pérez G. A. M., Acosta-Pulido J. A., González-Martin O., 2008, ApJ, 680, L17

Rickes M. G., Pastoriza M. G., Bonatto C., 2008, MNRAS, 384, 1427

Rickes M. G., Pastoriza M. G., Bonatto C., 2009, A&A, 505, 73

Rieke G. H., Lebofsky M. J., Thompson R. I., Low F. J., Tokunaga A. T., 1980, ApJ, 238, 24

Riffel R., Pastoriza M. G., Rodríguez-Ardila A., Maraston C., 2007, ApJ, 659, L103

Riffel R., Pastoriza M. G., Rodríguez-Ardila A., Maraston C., 2008, MNRAS, 388, 803

Riffel R., Pastoriza M. G., Rodríguez-Ardila A., Bonatto C., 2009, MNRAS, 400, 273

Riffel R. A., Storchi-Bergmann T., Riffel R., Pastoriza M., 2010, ApJ, 713, 469

Rodighiero G., Cimatti A., Franceschini A., Brusa M., Fritz J., Bolzonella M., 2007, A&A, 470, 21

Salpeter E. E., 1955, ApJ, 121, 161

Saraiva M. F., Bica E., Pastoriza M. G., Bonatto C., 2001, A&A, 376, 43

Scalo J. M., 1986, in de Loore C. H., Willis A. J., Laskarides P., eds, Proc. IAU Symp. Vol. 116, Luminous Stars and Associations in Galaxies. Reidel, Dordrecht, p. 451

Schaller G., Schaerer D., Meynet G., Maeder A., 1992, A&AS, 96, 269

Schmitt H. R., Bica E., Pastoriza M. G., 1996, MNRAS, 278, 965

Schulz J., Fritze U., Moller C. S., Fricke K. J., 2002, A&A, 392, 1

Searle L., Zinn R., 1978, ApJ, 225, 357

Serra P., Trager S. C., 2007, MNRAS, 374, 769

Silva L., Granato G. L., Bressan A., Danese L., 1998, ApJ, 509, 103

Thomas D., Davies R. L., 2006, MNRAS, 366, 510

Thomas D., Maraston C., Bender R., Mendes de Oliveira C., 2005, ApJ, 621, 673

Trager S. C., Faber S. M., Worthey G., González J. J., 2000a, AJ, 119, 1645

Trager S. C., Faber S. M., Worthey G., González J. J., 2000b, AJ, 120, 165

van der Wel A., Franx M., Wuyts S., van Dokkum P. G., Huang J., Rix H.-W., Illingworth G. D., 2006, ApJ, 652, 97

Vazdekis A., Arimoto N., 1999, ApJ, 525, 144

Westera P., Lejeune T., Buser R., Cuisinier F., Bruzual G., 2002, A&A, 381, 524

White S. D. M., 1984, ApJ, 286, 38

Worthey G., 1994, ApJS, 95, 107

APPENDIX A: HOW TO USE THE PaASP FORM

In this appendix we provide details how to use the PaASP form. PaASP is available at http://www.if.ufrgs.br/~riffel/software.html.

(i) Bin your synthesis results (x_j) into three population vectors: young, intermediate and old ages. For more information on the definition of the populations vectors see Cid Fernandes et al. (2004, 2005) and Riffel et al. (2009).

(ii) Select the representative age of each vector, for example: 5 Myr for young, 200 Myr for intermediate and 13 Gyr for old. Tip: take as the representative population the ages of x_j with the largest contribution in each bin.

(iii) Put the percentage contribution (only integers and sum equal to 100 per cent are allowed) of each age in the form, select the normalization point and submit it.

(iv) You will be redirected to the results query page. There your inputs are marked in red and the propagated results over all λs (see text) are shown. You can also download the file with a table with propagation results for all the results of equation (4), in fractions of 1 per cent for your query.

(v) The first three columns of the table are the input fractions for a given normalization point and for three ages, which are specified in the header (first and second lines). The next columns are the propagation of the results for all λs. Note that the results are given in three lines blocks: young, intermediate and old fractions, respectively.

PaASP is freely distributed and is supported by Brazilian funding agencies CAPES and CNPq. An acknowledgement for the use would be appreciated.

This paper has been typeset from a T<small>E</small>X/L<small>A</small>T<small>E</small>X file prepared by the author.